

# Fabrication of high thermal conductivity Cu/diamond composites at ambient temperature and pressure

Cite as: AIP Advances 9, 085309 (2019); <https://doi.org/10.1063/1.5111416>

Submitted: 26 May 2019 . Accepted: 05 August 2019 . Published Online: 13 August 2019

S. Arai, and  M. Ueda

## COLLECTIONS

Paper published as part of the special topic on [Chemical Physics](#), [Energy, Fluids and Plasmas](#), [Materials Science](#) and [Mathematical Physics](#)



View Online



Export Citation



CrossMark

## ARTICLES YOU MAY BE INTERESTED IN

[Effect of titanium and zirconium carbide interphases on the thermal conductivity and interfacial heat transfers in copper/diamond composite materials](#)

AIP Advances 9, 055315 (2019); <https://doi.org/10.1063/1.5052307>

[Film deposition by thermal laser evaporation](#)

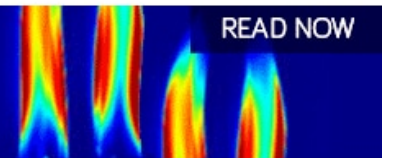
AIP Advances 9, 085310 (2019); <https://doi.org/10.1063/1.5111678>

[Effects of disorder state and interfacial layer on thermal transport in copper/diamond system](#)

Journal of Applied Physics 117, 074305 (2015); <https://doi.org/10.1063/1.4906958>

AIP Advances  
Fluids and Plasmas Collection

READ NOW



# Fabrication of high thermal conductivity Cu/diamond composites at ambient temperature and pressure

Cite as: AIP Advances 9, 085309 (2019); doi: 10.1063/1.5111416

Submitted: 26 May 2019 • Accepted: 5 August 2019 •

Published Online: 13 August 2019



View Online



Export Citation



CrossMark

S. Arai<sup>a)</sup> and M. Ueda 

## AFFILIATIONS

Department of Materials Chemistry, Faculty of Engineering, Shinshu University, Nagano, 380-8553, Japan

<sup>a)</sup>Corresponding author: [araisun@shinshu-u.ac.jp](mailto:araisun@shinshu-u.ac.jp)

## ABSTRACT

High thermal conductivity Cu/diamond composites were produced at ambient temperature and pressure using an electrodeposition technique, employing various diamond particle sizes in the range of 10 to 230  $\mu\text{m}$ . The microstructures of the resulting composites were analyzed by scanning electron microscopy and their thermal conductivities were assessed using a Xenon flash instrument. The theoretical thermal conductivities of these materials were calculated based on the Hasselman-Johnson equation and compared with the experimentally determined values. The Cu/diamond composites produced in this work were found to exhibit compact textures without any gaps between the Cu matrix and the diamond particles, and the experimental thermal conductivities were in good agreement with the theoretical values. The specimen containing 61 vol.% of 230  $\mu\text{m}$  diameter diamond particles had the highest conductivity of  $662 \text{ W K}^{-1} \text{ m}^{-1}$ , which is 1.6 times that of pure Cu (ca.  $400 \text{ W K}^{-1} \text{ m}^{-1}$ ).

© 2019 Author(s). All article content, except where otherwise noted, is licensed under a Creative Commons Attribution (CC BY) license (<http://creativecommons.org/licenses/by/4.0/>). <https://doi.org/10.1063/1.5111416>

Diamond exhibits very high thermal conductivity, second only to that of carbon nanotubes (CNTs).<sup>1–6</sup> However, due to their unique structure, the thermal conductivity of CNTs is also highly anisotropic,<sup>2</sup> such that the conductivity is greatest along the axial direction. In contrast, diamond particles typically have a granular morphology and exhibit a more isotropic thermal conductivity. For this reason, diamond particles are expected to be applicable as raw materials for the preparation of high thermal conductivity composite materials. In particular, metal/diamond composites could potentially be used as heat sink and heat dispersion materials, and there has been much research regarding the fabrication of composites comprising diamond together with Al,<sup>7,8</sup> Ag<sup>9</sup> or Cu.<sup>10–17</sup> Sintering and infiltration have traditionally been used to form such materials, although both require the application of extremely high temperatures and pressures. Moreover, metals such as Ag and Cu in the molten state are not able to readily wet diamond. Consequently, gaps or cracks tend to form between the metal matrix and the diamond particles in the composite, such that the resulting thermal conductivity is actually lower than that of the original metal. Both wettability and thermal conductivity can be improved by pre-coating the

diamond particles with the metal,<sup>2,18–22</sup> although the thermal resistance between the metal matrix and the diamond particles is increased due to the metal coating on the diamond particles and still requires the application of extremely high temperatures and pressures.

Electrodeposition could potentially be used to form metal layers on solid materials at ambient temperature and pressure, and so might be advantageous. However, there have been few reports concerning the thermal conductivity of metal/diamond composite materials fabricated using this technique. In the present study, we produced Cu/diamond composites by electrodeposition and evaluated the thermal conductivities of the resulting films. Cu was selected as the matrix because the electrodeposition of this metal from an aqueous solution can be readily accomplished without the use of toxic chemicals, and because Cu has the second highest thermal conductivity among the metallic elements (after Ag).

Commercially-available single crystal diamond particles with various mean sizes (MMP series with 10, 25 and 45  $\mu\text{m}$  sizes and SXD series with 230  $\mu\text{m}$  size, Changsha Xinye Co., Ltd.) were used.

An aqueous solution containing 0.85 M  $\text{CuSO}_4 \cdot 5\text{H}_2\text{O}$  and 0.55 M  $\text{H}_2\text{SO}_4$  was employed as the Cu plating bath. Electrodeposition was carried out at room temperature and atmospheric pressure under galvanostatic condition ( $5 \text{ mA cm}^{-2}$ ), using a pure Cu plate together with a stainless steel plate, serving as the cathode. The diamond content and thermal properties of the test specimens were assessed after exfoliation of these samples from the stainless steel cathode. A pure Cu plate was used as the anode. The electrolytic cell was constructed of an acrylic resin and its internal dimensions were  $3.5 \times 7 \times 6 \text{ cm}$ . The electrodes were arranged horizontally, with the cathode at the bottom, having an exposed surface area of  $3 \times 6 \text{ cm}$ . The diamond particles were added to the Cu plating bath and dispersed homogeneously using a stir bar, after which they were left undisturbed to precipitate on the cathode. Since the diamond particles used in this study have relatively large sizes ( $> 10 \mu\text{m}$ ), they dispersed homogeneously without any aggregations and precipitated uniformly on the cathode. After that, electrodeposition was performed such that the gaps between the precipitated diamond particles were filled with Cu. The masses of the 10, 25, 45 and  $230 \mu\text{m}$  diamond particles added to the bath were 0.11, 0.28, 0.50 and 2.53 g, respectively, which correspond to approximately two layers of particles on the cathode. The respective quantities of electrical charge sent through the cell were 54, 135, 243 and  $1240 \text{ C cm}^{-2}$ . In addition, a thicker specimen was fabricated using a 5.1 g mass of the  $230 \mu\text{m}$  diamond particles in conjunction with a charge density of  $2500 \text{ C cm}^{-2}$ . For comparison purposes, pure electrodeposited Cu samples were also produced at  $5 \text{ mA cm}^{-2}$  ( $54 \text{ C cm}^{-2}$ ). The experimental setup for the fabrication of Cu/diamond composites using electrodeposition is shown in Fig. 1.

The diamond content (in terms of volume percentage) in each composite was determined by directly weighing the specimens after the removal of the Cu matrix with  $\text{HNO}_3$ . The surface and cross-sectional morphologies of the composites were examined

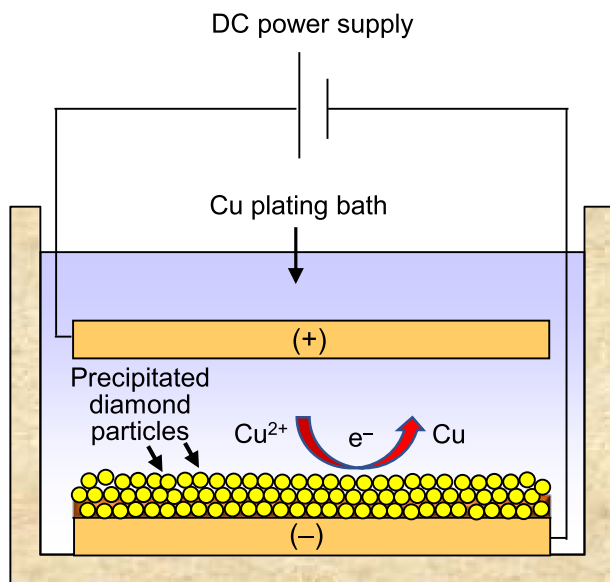


FIG. 1. Experimental setup for the fabrication of Cu/diamond composites using an electrodeposition technique.

using field-emission scanning electron microscopy (FE-SEM, SU-8000, Hitachi High Technology Co.), employing a cross-section polisher (SM-09010, JEOL Ltd.) to prepare the cross-sectional samples. The thermal diffusivity ( $\alpha$ ) of each specimen was measured with a xenon laser flash thermal properties analyzer (LFA 447-2 Nanoflash, Netzsch Co., Ltd.). The  $\alpha$  values of the Cu/diamond composite samples made with 10, 25 and  $45 \mu\text{m}$  diamond particles were determined in the thin film, plain mode, while the specimen made with  $230 \mu\text{m}$  particles was assessed in the bulk, normal mode. The density ( $\rho_{comp}$ ) and specific heat capacity ( $C_{comp}$ ) of each composite were calculated using the equations<sup>10,13</sup>

$$\rho_{comp} = \rho_{dia} \cdot V_{dia} + \rho_{Cu} \cdot V_{Cu} \quad (1)$$

and

$$C_{comp} = \frac{C_{dia} \cdot V_{dia} \cdot \rho_{dia} + C_{Cu} \cdot V_{Cu} \cdot \rho_{Cu}}{\rho_{comp}}, \quad (2)$$

respectively, where  $\rho_{dia}$  and  $\rho_{Cu}$  are the densities of diamond ( $3520 \text{ kg m}^{-3}$ ) and Cu ( $8940 \text{ kg m}^{-3}$ ),  $V_{dia}$  and  $V_{Cu}$  are the experimentally determined volume percentages of diamond and Cu, and  $C_{dia}$  and  $C_{Cu}$  are the specific heat capacities of diamond ( $512 \text{ J kg}^{-1} \text{ K}^{-1}$ ) and Cu ( $385 \text{ J kg}^{-1} \text{ K}^{-1}$ ), respectively.

The thermal conductivity ( $\lambda_{comp}$ ) of each sample was calculated as

$$\lambda_{comp} = \alpha \cdot \rho_{comp} \cdot C_{comp}. \quad (3)$$

Simulations of the thermal conductivities of the various Cu/diamond composites were also carried out, using the Hasselman-Johnson

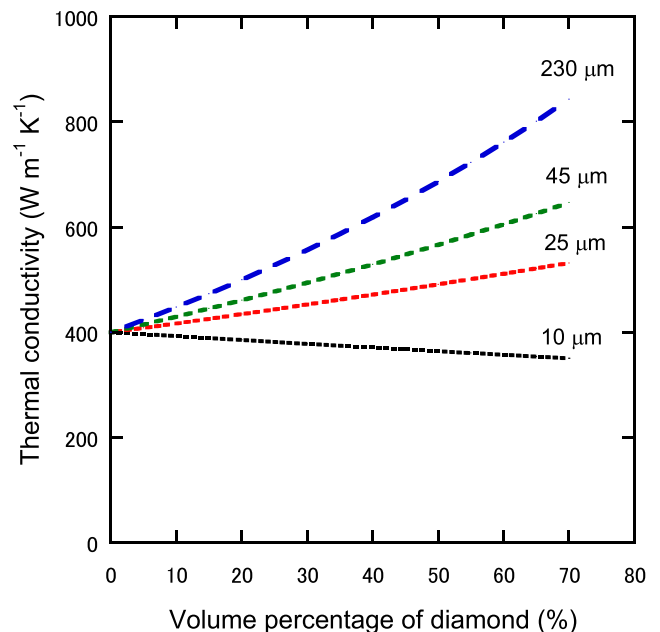
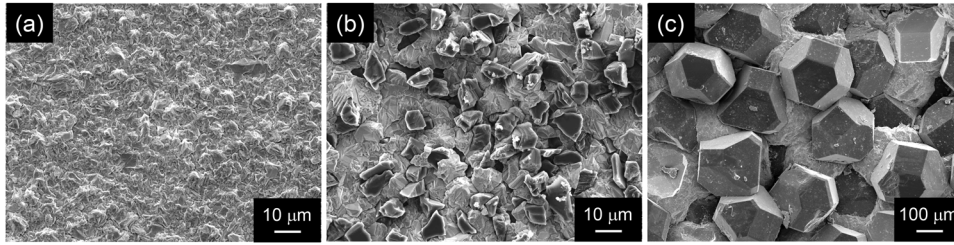
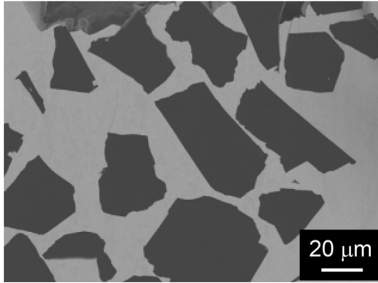


FIG. 2. Theoretical curves of thermal conductivities of Cu/diamond composites with various diamond particle diameters as a function of volume fraction of diamond. Thermal conductivities of copper and diamond are assumed to be  $400 \text{ W m}^{-1} \text{ K}^{-1}$  and  $1300 \text{ W m}^{-1} \text{ K}^{-1}$ , respectively. The boundary conductance between copper matrix and diamond particles is assumed to be  $8.86 \times 10^8 \text{ W m}^{-2} \text{ K}^{-1}$ .



**FIG. 3.** Surface SEM images of (a) a pure copper film, and of Cu/diamond composites made with (b) 10  $\mu\text{m}$  and (c) 230  $\mu\text{m}$  diamond particles, produced using electrodeposition.



**FIG. 4.** Cross-sectional SEM image of a Cu/diamond composite made with 45  $\mu\text{m}$  diamond particles.

equation<sup>23</sup>

$$\lambda_{sim} = \lambda_{Cu} \left\{ \frac{2 \left( \frac{\lambda_{dia}}{k_{Cu}} - \frac{\lambda_{dia}}{ah_c} - 1 \right) V_{dia} + \frac{\lambda_{dia}}{\lambda_{Cu}} + \frac{2\lambda_{dia}}{ah_c} + 2}{\left( 1 - \frac{\lambda_{dia}}{\lambda_{Cu}} + \frac{\lambda_{dia}}{ah_c} \right) V_d + \frac{\lambda_{dia}}{\lambda_{Cu}} + \frac{2\lambda_{dia}}{ah_c} + 2} \right\}, \quad (4)$$

where  $\lambda_{sim}$  is the simulated thermal conductivity of the Cu/diamond composite,  $\lambda_{dia}$  is the thermal conductivity of diamond,  $\lambda_{Cu}$  is the thermal conductivity of Cu,  $a$  is the mean radius of the diamond particles,  $V_{dia}$  is the volume percentage of the diamond particles, and  $h_c$  is the boundary conductance between the Cu matrix and diamond particles. In this simulation,  $\lambda_{dia}$ ,  $\lambda_{Cu}$  and  $h_c$  were assumed to be  $1300 \text{ W m}^{-1} \text{ K}^{-1}$ ,<sup>10,18</sup>  $400 \text{ W m}^{-1} \text{ K}^{-1}$  and  $8.86 \times 10^8 \text{ W m}^{-2} \text{ K}^{-1}$ ,<sup>24</sup> respectively.

Figure 2 plots the simulated thermal conductivity values for the Cu/diamond composites with various diameters of diamond particles used in this study. When using 10  $\mu\text{m}$  diamond particles, the thermal conductivity of the composite decreases as the diamond

volume percentage increases. In contrast, the thermal conductivities of the specimens containing particles 25  $\mu\text{m}$  or larger in size increase with increases in the volume percentage of diamond. The thermal conductivities of the Cu/diamond composites also increase with increasing diamond particle size.

Figure 3 presents surface SEM images of composites fabricated by electrodeposition. For comparison purposes, the surface SEM image of a pure Cu specimen is shown in Figure 3a. It is evident that the diamond particles were uniformly dispersed throughout the Cu matrices in the samples containing 45  $\mu\text{m}$  (Figure 3b) and 230  $\mu\text{m}$  (Figure 3c) diamond particles. Similar homogeneous distributions were evident in samples made using other sizes of diamond.

Figure 4 shows the cross-sectional SEM image of the Cu/diamond composite made with 45  $\mu\text{m}$  diamond particles, in which the dark areas are the diamond particles and the bright areas represent the Cu matrix. The electrodeposited Cu is seen to completely fill the spaces between diamond particles such that there are no gaps. Thus, electrodeposition evidently permitted the formation of dense Cu/diamond composites.

Table I summarizes the experimentally determined and theoretical thermal conductivities of the pure Cu and Cu/diamond composites. The theoretical values provided here were calculated using the Hasselman-Johnson relationship given above as Eq. 4. The measured thermal conductivity of the pure Cu is almost equal to the theoretical value, and the conductivities of the composites are also similar to the simulated values. Although the conductivity of the composite containing 230  $\mu\text{m}$  diamond particles ( $662 \text{ W m}^{-1} \text{ K}^{-1}$ ) is somewhat lower than the theoretical value ( $769 \text{ W m}^{-1} \text{ K}^{-1}$ ), it is 1.6 times higher than that of pure Cu ( $400 \text{ W m}^{-1} \text{ K}^{-1}$ ). As shown in Figure 4, the Cu/diamond composites had dense textures with no gaps between the diamond particles and Cu matrix, which is ideal. Consequently, the materials fabricated in this study would be expected to exhibit close to theoretical thermal conductivity values.

**TABLE I.** Thermal conductivity values of Cu/diamond composites.

Sample	Diamond particle size ( $\mu\text{m}$ )	Volume percentage of diamond (%)	Thermal conductivity: Measured ( $\text{W m}^{-1} \text{ K}^{-1}$ )	Thermal conductivity: Theoretical ( $\text{W m}^{-1} \text{ K}^{-1}$ )
Pure Cu	–	0	397	400
Cu/diamond	10	24	381	382
Cu/diamond	25	26	444	446
Cu/diamond	45	31	520	498
Cu/diamond	230	61	662	769

In conclusion, Cu/diamond composites with high thermal conductivities were fabricated at ambient temperature and pressure using an electrodeposition technique. Because these materials had dense textures and a lack of gaps between the diamond particles and the Cu matrices, they exhibited thermal conductivities that approached theoretical values. The composite made with 230  $\mu\text{m}$  diamond particles had an especially high thermal conductivity of  $662 \text{ W m}^{-1} \text{ K}^{-1}$ , which is 1.6 times that of pure Cu. Thus, the process used in this study is a useful means of synthesizing high thermal conductivity metal/diamond materials with potential applications as heat dissipation components.

## REFERENCES

- <sup>1</sup>C. Y. Ho, R. W. Powell, and P. E. Liley, *J. Phys. Chem. Data* **1**, 279 (1972).
- <sup>2</sup>A. M. Abyzov, S. V. Kindalov, and F. M. Shakhov, *J. Mater. Sci.* **46**, 1424 (2011).
- <sup>3</sup>S. Berber, Y. K. Kwon, and D. Tomaneck, *Phys. Rev. Lett.* **84**, 4613 (2000).
- <sup>4</sup>A. Cao and J. Qu, *J. Appl. Phys.* **112**, 013503 (2012).
- <sup>5</sup>C. H. Yu, L. Shi, Z. Yao, D. Y. Li, and A. Majumdar, *Nano Lett.* **5**, 1842 (2005).
- <sup>6</sup>P. Kim, L. Shi, A. Majumdar, and P. L. McEuen, *Phys. Rev. Lett.* **87**, 215502 (2001).
- <sup>7</sup>H. Feng, J. K. Yu, and W. Tan, *Mat. Chem. Phys.* **124**, 851 (2010).
- <sup>8</sup>K. Mizuuchi, K. Inoue, Y. Agari, Y. Morisada, M. Sugioka, M. Tanaka, T. Takeuchi, M. Kawahara, and U. Makino, *Compos. Part B* **42**, 1029 (2011).
- <sup>9</sup>M. T. Lee, M. H. Fu, J. L. Wu, C. Y. Chung, and S. J. Lin, *Diam. Relat. Mater.* **20**, 130 (2011).
- <sup>10</sup>K. Yoshida and H. Morigami, *Microelectron. Reliab.* **44**, 303 (2004).
- <sup>11</sup>L. Weber and R. Tavangar, *Scripta Mater* **57**, 988 (2007).
- <sup>12</sup>E. A. Ekimov, N. V. Suetin, A. F. Popovich, and V. G. Ralchenko, *Diamond Relat. Mater.* **17**, 838 (2008).
- <sup>13</sup>Y. H. Dong, X. B. He, R. U. Din, L. Xu, and X. H. Qu, *J. Mater. Sci.* **46**, 3862 (2011).
- <sup>14</sup>H. Bai, N. Ma, J. Lang, and C. Zhu, *J. Alloys Comp.* **580**, 382 (2013).
- <sup>15</sup>K. Raza and F. A. Khalid, *J. Alloys Comp.* **615**, 111 (2014).
- <sup>16</sup>H. Y. Wang and J. Tian, *Appl. Phys. A* **116**, 265 (2014).
- <sup>17</sup>P. Mankowski, A. Dominiak, R. Domanski, M. Kruszewski, and L. Ciupinski, *J. Therm. Anal. Calorim.* **116**, 881 (2014).
- <sup>18</sup>K. Chu, Z. Liu, C. Jia, H. Chen, X. Liang, W. Gao, W. Tian, and H. Guo, *J. Alloys Comp.* **490**, 453 (2010).
- <sup>19</sup>S. Ren, X. Shen, C. Guo, N. Liu, J. Zang, X. He, and X. Qu, *Compos. Sci. Technol.* **71**, 1550 (2011).
- <sup>20</sup>A. M. Abyzov, S. V. Kidalov, and F. M. Shakhov, *Appl. Therm. Eng.* **48**, 72 (2012).
- <sup>21</sup>X. Y. Shen, X. B. He, S. B. Ren, H. M. Zhang, and X. H. Qu, *J. Alloys Comp.* **529**, 134 (2012).
- <sup>22</sup>Q. Kang, X. He, S. Ren, L. Zhang, M. Wu, T. Liu, Q. Liu, C. Gu, and X. Qu, *J. Mater. Sci.* **48**, 6133 (2013).
- <sup>23</sup>D. P. H. Hasselman and L. F. Johnson, *J. Comp. Mater* **21**, 508 (1987).
- <sup>24</sup>H. Wang, Y. Xu, M. Shimono, Y. Tanaka, and M. Yamazaki, *Mater. Trans.* **48**, 2349 (2007).